A Novel Scheme to Reduce Power Supply Noise for High-Quality At-Speed Scan Testing

Xiaoqing Wen, Kohei Miyase, Seiji Kajihara, Tatsuya Suzuki, Yuta Yamato,
Patrick Girard, Yuji Ohsumi, Laung-Terng Wang

A Novel Scheme to Reduce Power Supply Noise for High-Quality At-Speed Scan Testing

Xiaoqing Wen [1], Kohei Miyase [1], Seiji Kajihara [1], Tatsuya Suzuki [1], Yuta Yamato [1], Patrick Girard [2]
Yuji Ohsumi [3], and Laung-Terng Wang [4]

[1] Kyushu Institute of Technology, Iizuka 820-8502, Japan
[2] LIRMM, 161 rue Ada, 34392 Montpellier cedex 05, France
[3] Hibikino R&D Center, DNP Co. Ltd., Kitakyushu 808-0135, Japan
[4] SynTest Technologies, Inc., 505 S. Pastoria Ave., Sunnyvale, CA 94086, USA

Abstract

*High-quality at-speed scan testing, characterized by high small-delay-defect detecting capability, is indispensable to achieve high delay test quality for DSM circuits. However, such testing is susceptible to yield loss due to excessive power supply noise caused by high launch-induced switching activity. This paper addresses this serious problem with a novel and practical post-ATPG X-filling scheme, featuring (1) a test relaxation method, called **path keeping X-identification**, that finds don't-care bits from a fully-specified transition delay test set while preserving its delay test quality by keeping the longest paths originally sensitized for fault detection, and (2) an X-filling method, called **justification-probability-based fill (JP-fill)**, that is both effective and scalable for reducing launch-induced switching activity. This scheme can be easily implemented into any ATPG flow to effectively reduce power supply noise, without any impact on delay test quality, test data volume, area overhead, and circuit timing.*

1. Introduction

Shrinking feature size, growing circuit complexity, increasing clock speed, and decreasing power supply voltage have made timing-related defects, usually of small delays, the dominant failure mechanism in the deep submicron (DSM) era [1]. As a result, **high-quality delay testing**, characterized by high small-delay-defect detecting capability, is required in order to reduce the defect level of DSM circuits [2].
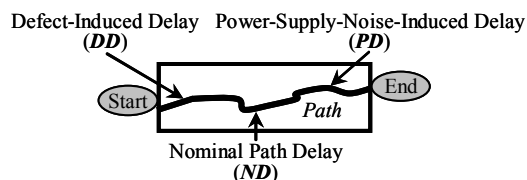
1.1 At-Speed Scan Testing

Delay testing is mostly conducted by **at-speed scan testing** [3]. This is due to its strong fault diagnosis support, easy implementation, and high fault coverage.

As illustrated in Fig. 1 (a), the essence of at-speed scan testing is to **launch** a transition at the start-point of a path (FF output) and **capture** its response at the end-point of the path (FF input) at the system speed. That is, the **test cycle** (*T*) is at-speed in order to directly check the delay of the path. As shown in Fig. 1 (b), a path may have three types of possible delays: **nominal path delay** (*ND*), **defect-induced delay** (*DD*), and **power-supply-noise-induced delay** (*PD*). A chip is identified to be defective if $ND + DD + PD > T$, that will cause an incorrect logic value to be loaded into the end-point FF due to the unsatisfied timing requirement.
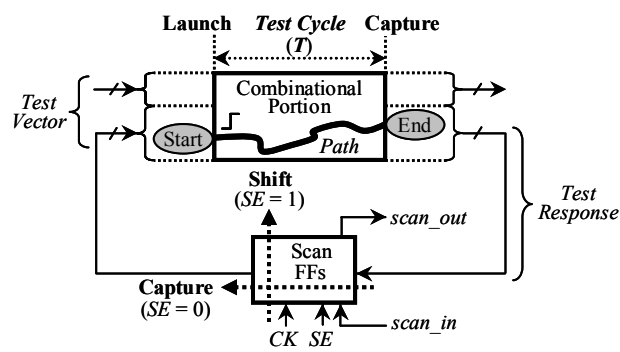
(a) Basic concept

(b) Types of possible delay

Fig. 1 At-Speed Scan Testing.

The launch of transitions in at-speed scan testing can be realized by either the **launch-off-shift** (**LOS**) through a shift pulse (*SE* = 1) or the **launch-off-capture** (**LOC**) scheme through a capture pulse (*SE* = 0) [3]. This paper focuses on LOC as shown in Fig. 2, since it is widely applied due to the use of a slow *SE* signal and conventional scan FFs.
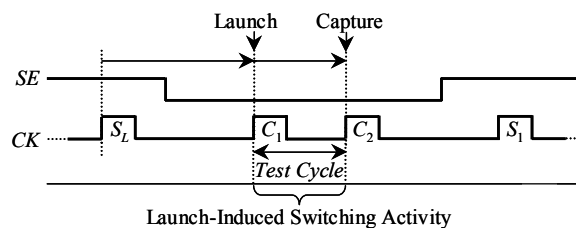
Fig. 2 Launch-off-Capture (LOC) Scheme.

1.2 High-Quality At-Speed Scan Testing

The quality of at-speed testing is measured by defect level (the fraction of defective chips passing a test), which depends on test vectors and test timing [4], as illustrated in Fig. 3.

Fig. 3 shows a defect with delay size *s*. Among paths passing through the defect spot, p_1 is the longest sensitized path while p_2 is the actual longest path in function mode.

Clearly, T_{mgn} is the maximum redundant delay size for the defect spot, while T_{det} is the minimum detectable delay size for the defect spot under the given test set. Note that $T_{SC} = T_{TC}$ in at-speed scan testing.
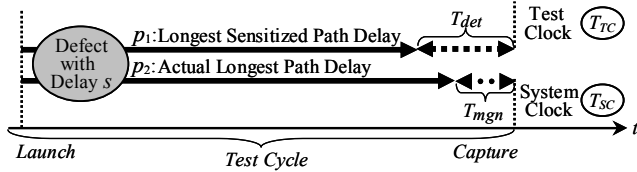

Fig. 3 Detection Condition in Delay Testing.

If the delay size s is non-negligibly small ($T_{mgn} < s < T_{det}$), test escape occurs since the defect can not be detected by the sensitized path ($s < T_{det}$) but may cause a functional problem ($s > T_{mgn}$). Since such small-delay defects are dominant in DSM circuits [1, 4], the capability to detect them determines the quality of at-speed scan testing.

Generally, in order to achieve high-quality at-speed scan testing, it is necessary to narrow the gap between T_{mgn} and T_{det} so as to reduce the occurrence of test escapes. Since T_{mgn} is fixed by design, the only choice is to reduce T_{det}.

One approach for reducing T_{det} is to tighten the test clock (moving T_{TC} in Fig. 3 to the left). This is referred to as *pattern-dependent timing* or *faster-than-at-speed scan testing* [5, 6]. The basic idea is to group tests according to their lengths, and properly tighten the test clock for each group so that the corresponding T_{det} is reduced in effect.

Another approach for reducing T_{det} is to increase the length of sensitized paths by biasing ATPG towards sensitizing long paths for fault detection. This can be directly achieved by *path delay test generation* [3], but the number of paths is prohibitively high. In practice, the transition delay fault model [3] is widely used since its fault count is manageable in that it is proportional to the number of nodes in a circuit. However, *timing-aware transition delay test generation* is needed in order to sensitize as long paths as possible in transition delay fault detection, for the purpose of achieving high small-delay-defect detecting capability [2, 7-9].

From Fig. 3, it is also clear that the delay test quality of a transition delay test set for at-speed scan testing depends on the set of longest paths sensitized for fault detection [2, 4, 9]. In this paper, this set of paths is called the *characteristic path set* (*CPS*) of the transition delay test set.

1.3 Power Supply Noise

When switching activity occurs in a circuit, current flows through the equivalent RLC network, resulting in IR and $L{\cdot}di/dt$ voltage drop at logic cells. This is called *power supply noise* [10], which has severe impact on high-quality at-speed scan testing due to the following factors:

• *High Launch-Induced Switching Activity*: The switching activity caused by the launch operation (Fig. 1 (a)) is much higher than that of functional operation [11-13]. This

results in voltage drop at cells, increasing cell delays and thus path delay. This means larger *PD* in Fig. 1 (b).

• *Long Path Sensitization*: Long paths are sensitized for fault detection in high-quality at-speed scan testing. This means larger *ND* in Fig. 1 (b).

• *Short Test Cycle*: The time between launch and capture is short. This means smaller *T* in Fig. 1 (a).

All these factors cause $ND + PD > T$ to occur frequently, which often makes a normal circuit to fail in testing. Since this results in power-supply-noise-induced yield loss, power supply noise has become a critical issue in high-quality at-speed scan testing [14, 15].

The impact of power supply noise can be analyzed in terms of voltage drop and/or delay increase. Approximation methods [10, 14, 15] are often used since accurate analysis is time-consuming. Their results are used to guide test generation [14] or reduce the number of target test vectors before accurate analysis is conducted for sign-off [15].

Power supply noise reduction is more important, which requires to lower launch-induced switching activity. For LOC-based at-speed scan testing, this means that switching activity due to the first capture (C_1 in Fig. 2) should be reduced. Three approaches are available for this purpose:

(1) *Test Clocking*: One-hot and *multi-capture* clocking schemes can reduce the number of clock domains that capture simultaneously [3].

(2) *Circuit Change*: DFT methods, such as *partial capture* [16], can be used to allow only part of a circuit to capture.

(3) *Test Generation*: Switching activity can be directly reduced by generating proper logic values in ATPG [17, 18], assigning logic values to don't care bits by in-ATPG or post-ATPG *X*-filling [19-24], and test compaction [25].

Generally, the test generation approach is preferable. Especially, *post-ATPG X-filling* is now widely used in practice for power supply noise reduction [22, 24], since it can be easily implemented into any ATPG flow, without any impact on test data volume, area overhead, and circuit timing. More details will be described below.

1.4 Motivation

Post-ATPG *X*-filling for power supply noise reduction is illustrated in Fig. 4, which consists of two major steps:

(1) *Test Relaxation*: This is the process to identify don't care bits, referred to as *X-bits*, from a set of fully-specified *test vectors* under the condition that the property of the test set, e.g. its fault coverage, is preserved [26-28]. The result of this step is a set of *test cubes* with *X*-bits.

(2) *X-Filling*: This is the process to assign logic values to the *X*-bits in a test cube so that the resulting fully-specified test vector has low launch-induced switching activity. Logic values can be determined by minimizing either the Hamming distance between a test vector and its response at FFs [19-22] or the weighted node transition count in a circuit [23].
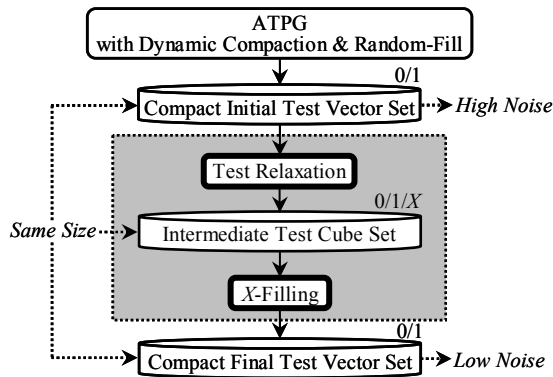
Fig. 4 Post-ATPG *X*-Filling for Power Supply Noise Reduction.

The major advantage of post-ATPG *X*-filling is that it reduces power supply noise without inflating test data volume. As shown in Fig. 4, this is achieved by using test relaxation to obtain *X*-bits from a compact initial test vector set generated by ATPG with ***dynamic compaction*** and ***random-fill*** [3]. Forcing ATPG to leave unspecified bits as *X*-bits without using them to improve detection efficiency will result in much larger test sets. Note that, although over 90% of bits may remain unspecified even after dynamic compaction, not conducting random-fill on them will still significantly increase test data volume [21, 22].

However, previous post-ATPG *X*-filling methods for power supply noise reduction suffer from two major problems with respect to high-quality at-speed scan testing:

Problem-1: *Test Quality Degradation in Test Relaxation*

Previous test relaxation methods [26-28] can be readily extended for the transition delay fault model to identify *X*-bits from a fully-specified transition delay test set while preserving its fault coverage. However, all of them totally ignore the paths sensitized for transition delay fault detection. Consequently, *X*-filling the test cubes obtained by such test relaxation methods results in a final test set with different sensitized paths. As illustrated in Fig. 5, if the initial test set has high delay test quality characterized by its characteristic path set, the delay test quality of the final test set can be very different, usually low, since it has a different characteristic path set with possibly shorter paths. Therefore, test relaxation ignoring path sensitization information may result in significant delay test quality degradation.
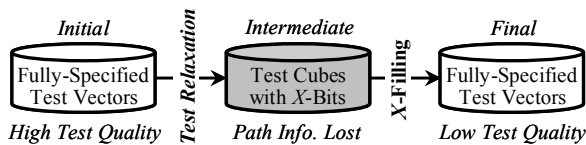

Fig. 5 Test Quality Degradation.

Problem-2: *Effectiveness vs. Scalability in X-Filling*

Ideal *X*-filling should be both ***effective*** in reducing launch-induced switching activity as much as possible and ***scalable*** to large circuits in terms of short CPU time. Previous *X*-filling methods use time-consuming justification to maximize effectiveness [19, 21] or aggressive approximation

based on signal probability to maximize scalability [22]. As illustrated in Fig. 6, there is a need for more balanced *X*-filling, which is highly effective and sufficiently scalable, especially for high-quality at-speed scan testing of industrial circuits. This is due to the facts of (1) growing circuit scale, (2) less *X*-bits identified by test relaxation since more properties, e.g. fault coverage as well as delay test quality, should be preserved, and (3) the need of using part of *X*-bits for other purposes, such as test compression [3].
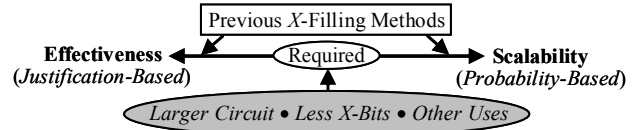

Fig. 6 Effectiveness vs. Scalability.

1.5 Contributions

This paper tackles the above problems with a new post-ATPG *X*-filling scheme. (1) Problem-1 is solved by a unique test relaxation method, called ***path-keeping X-identification***, which finds *X*-bits from a set of fully-specified transition delay test vectors while keeping the set of longest paths, i.e. characteristic path set, sensitized by the original fully-specified test vectors for fault detection. This preserves the delay test quality, as well as the fault coverage, of the original test set. (2) Problem-2 is solved by an effective and scalable *X*-filling method, called ***justification-probability-based fill*** (***JP-fill***), in which techniques based on justification and probability are used selectively, depending on how *X*-bits appear at the inputs and outputs of corresponding flip-flops. This achieves effectiveness and scalability in a more balanced manner.

The new post-ATPG *X*-filling scheme can be easily implemented into any ATPG flow to effectively reduce power supply noise without any impact on delay test quality, test data volume, area, and timing. This greatly improves the applicability of high-quality at-speed scan testing.

1.6 Organization

The rest of the paper is organized as follows: Section 2 describes the background. Section 3 outlines the new scheme. Sections 4 and 5 present the details of path-keeping *X*-identification and JP-fill, respectively. Section 6 shows experimental results, and Section 7 concludes the paper.

2. Background

We first discuss issues related to delay test quality. Then, we review test relaxation and *X*-filling in detail.

2.1 Delay Test Quality

A. Characteristic Path Set

As illustrated in Fig. 1 (a), scan-based delay testing for a path is conducted by creating a ***start transition*** at the start-point of the path and establishing a ***sensitization path*** to propagate the transition effect to the end-point of the path.

A sensitization path can be established either explicitly by *path delay test generation* or implicitly by *transition delay test generation* [3]. In path delay test generation, a target path is explicitly specified and test generation is conducted to sensitize it directly. In transition delay test generation, a slow-to-rise or slow-to-fall transition fault is assumed at a node, which by itself does not specify any path. As illustrated in Fig. 7, transition delay test generation then tries to establish an *excitation path* from the start-point of the path to the fault site for creating a proper transition at the fault site and a *propagation path* for passing the fault effect from the fault site to the end-point of the path. This way, a sensitization path, which is the combination of the excitation path and the propagation path, is established implicitly. In this paper, we focus on transition delay test generation since it is more widely used in practice.
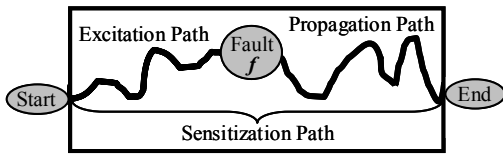

Fig. 7 Paths in Transition Delay Test Generation.

Definition 1: Suppose that V is a transition delay test set and $\{f_1, f_2, ..., f_d\}$ is the set of all transition delay faults detected by V. The longest path sensitized by vectors in V for a fault f_i is called the *characteristic path* of the fault f_i under the test set V, denoted by $CP(f_i, V)$. The set of all characteristic paths under V, $\{CP(f_i, V) \mid i = 1, 2, ..., d\}$, is called the *characteristic path set* of V, denoted by $CPS(V)$.

For example, a test set V can detect two faults: f_a and f_b. Suppose that f_a can be detected with three paths: $p_{a1}(7)$, $p_{a2}(9)$, $p_{a3}(5)$, while f_b can be detected with two paths: $p_{b1}(5)$, $p_{b2}(3)$. Here, the number in the parenthesis is the length of the corresponding path. In this case, $CPS(V) = \{p_{a2}, p_{b1}\}$.

There are two approaches for obtaining the $CPS(V)$ for a transition delay test set V, depending on what type of ATPG, *timing-ignoring* or *timing-aware*, is used to generate V.

Case-1 (*Timing-Ignoring ATPG*): In this case, a transition delay fault f is declared "*detected*" by a test vector $v \in V$ whenever a sensitization path is established, no matter how short the path may be [3]. As a result, there is no guarantee that the path sensitized by v is the longest for the detection of f under the whole test set V. Therefore, timing-based simulation is needed in order to find the longest sensitization path for each detected fault in order to obtain $CPS(V)$.

Case-2 (*Timing-Aware ATPG*): In this case, the excitation and propagation paths by a test vector v are made as long as possible to detect a fault f [2, 7-9]. As a result, the path sensitized by v is usually the longest for the detection of f under the whole test set V [2, 9]. Therefore, it is only necessary to simply record the sensitization path at the time when the corresponding fault f is detected in test generation. That is, $CPS(V)$ is obtained as a by-product of timing-aware ATPG, and post-ATPG timing-simulation is not needed.

B. Delay Test Quality Metric

Generally, the delay test quality of a transition delay test set can be quantified by the *Statistical Delay Quality Level* (*SDQL)* metric [4]. The SDQL value for a transition delay test set V, denoted by $SDQL(V)$, is defined as

$$SDQL(V) = \sum_{i=1}^{n} \int_{Tmgn(fi)}^{Tdet(fi,V)} F(s)\, ds$$

where the set of all possible faults is $\{f_1, f_2, ..., f_n\}$, and $F(s)$ is the delay defect distribution function, i.e. the probability of a defect having the delay size of s. In addition, $T_{mgn}(f_i)$ and $T_{det}(f_i, V)$ are defined as follows [4]:

• $T_{mgn}(f_i)$ is the maximum redundant delay size with respect to fault f_i. As shown in Fig. 3, $T_{mgn}(f_i) = T_{SC}$ − (the delay of the actual longest path passing through f_i in function mode), where T_{SC} is the system clock period. Note that $T_{mgn}(f_i)$ is determined by design, and is independent of the test set V.

• $T_{det}(f_i, V)$ is the minimum detectable delay size with respect to fault f_i by the test set V. If f_i is undetected, $T_{det}(f_i, V) = \infty$; otherwise, as shown in Fig. 3, $T_{det}(f_i, V) = T_{TC}$ − (the delay of $CP(f_i, V)$), where T_{TC} is the test clock period. Note that $T_{det}(f_i, V)$ is determined by $CP(f_i)$, which depends on the test set V. Also note that $T_{SC} = T_{TC}$ in at-speed scan testing.

Thus, it is clear that the delay test quality of a transition delay test set V, measured by $SDQL(V)$, is determined by $CPS(V)$, if the test timing (the relation between T_{SC} and T_{TC}) and the delay defect distribution $F(s)$ are given. Generally, the longer the characteristic paths in $CPS(V)$, the higher the delay test quality of the transition delay test set V.

C. Test Quality Preservation

Definition 2: Suppose that V_1 and V_2 are two transition delay test sets, both detecting faults $f_1, f_2, ..., f_d$. If the length of $CP(f_i, V_2)$ is equal to or longer than that of $CP(f_i, V_1)$ for $i = 1, 2, ..., d$, it is said that $CPS(V_2) \geq CPS(V_1)$, and that the delay test quality of V_1 is *preserved* by V_2.

Since each characteristic path corresponds to a detected fault, $CPS(V_2) \geq CPS(V_1)$ means that the fault coverage and the delay test quality, measured by the SDQL metric [4], of V_2 are guaranteed to be no lower than those of V_1.

2.2 Test Relaxation

Test relaxation is the process of identifying *X*-bits from a set of fully-specified test vectors, while preserving its property, such as fault coverage. The resulting test cubes are often used for *test data reduction* [26], *test quality improvement* [28], and *test power/noise reduction* [19-25].

The major advantage of obtaining test cubes by test relaxation, instead of simply keeping unspecified bits in ATPG, is that a compact initial test set can be obtained through dynamic compaction and random-fill; otherwise, the test vector count may even double [22]. After a compact initial test set is generated, test relaxation can then be applied to obtain *X*-bits, usually as much as over 50% [27, 28].

Previous test relaxation methods are as follows: (1) *Bit-stripping* [26] changes one bit in a test vector into an *X*-bit and checks whether all the faults that are only detected by the vector are still detected. (2) The method in [27] identifies newly detected faults by a test vector, and marks all the lines whose values are required for each such fault to be detected. The unmarked input lines are set to *X*-bits. (3) *X-identification* [28] uses justification and implication to find input bits needed to detect each fault that is detected by only one test vector. Other input bits are turned into *X*-bits after adjustment is made so that all faults are detected.

However, all previous test relaxation methods only preserve fault coverage, but totally ignore the information on sensitization paths. Thus, the initial test set V_1 and the final test set V_2, obtained by *X*-filling the test cubes identified by such test relaxation, usually have different characteristic path sets, i.e. $CPS(V_1) \neq CPS(V_2)$. It is highly possible that $CPS(V_2)$ has shorter characteristic paths. As described in Section 2.1, this means that the delay test quality of the final test set V_2 is lower than that of the initial test set V_1.

Thus, test relaxation ignoring sensitization paths is not feasible for high-quality at-speed scan testing. This is tackled by a new test relaxation method, called *path-keeping X-identification*, whose details are described in Section 4.

2.3 *X*-Filling

X-filling is the process of properly assigning logic values to the *X*-bits in a test cube for achieving a specific goal. Here, the goal is to reduce launch-induced switching activity.

There are two major approaches to such *X*-filling, as shown in Figs. 8 and 9. Here, *c* is a test cube and *f(c)* is the response of the combinational portion *f*. Logic values need to be determined for the *X*-bits in *c*, such that the Hamming distance between $<p_1, q_1, r_1>$ and $<p_2, q_2, r_2>$ is reduced.

• *Justification-Based X-Filling* [19,21]: This is a multi-pass approach illustrated in Fig. 8. PPI-PPO bit-pairs of the form <logic value, *X*> are processed first, followed by those of the form <*X*, *X*>, one at a time. Here, $<p_1, p_2>$ is processed first by justifying 0 on p_2 since p_1 has 0. Suppose that this is achieved by setting 1 to *a*. Then, bit-pairs of the form <*X*, *X*> are processed. Note that one such bit-pair may require two passes of justification. For example, for $<r_1, r_2> = <X, X>$, 1 is first justified on r_2 and 1 is assigned to r_1. If this fails, 0 is then justified on r_2 and 0 is assigned to r_1. This approach is highly effective. However, it is less scalable due to long run time, especially for bit-pairs of the form <*X*, *X*>.
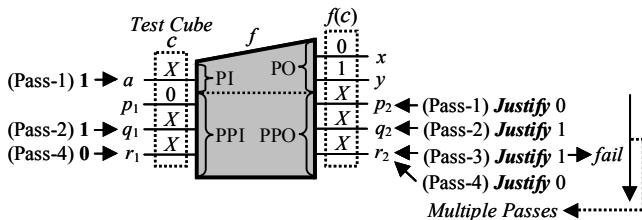

Fig. 8 Justification-Based *X*-Filling.

• *Probability-Based X-Filling* [22]: This is a single-pass approach illustrated in Fig. 9. The 0 and 1 probabilities of each node are first calculated by setting 0.50 as the 0 and 1 probabilities for each input *X*-bit and conducting probability propagation. Then, the logic value for a PPI *X*-bit is determined by using the relation between the 0 and 1 probabilities of its corresponding PPO *X*-bit. For example, (0.93, 0.07) on q_2 means that q_2 is likely to be 0, thus, it is reasonable to set 0 to q_1. This approach is highly scalable. However, its effect may be damaged by approximation in probability calculation. Especially, if the difference between the 0 and 1 probabilities at a PPO *X*-bit is negligibly small, e.g. (0.49, 0.51) on r_2, logic value determination for its corresponding PPI *X*-bit becomes highly inaccurate.
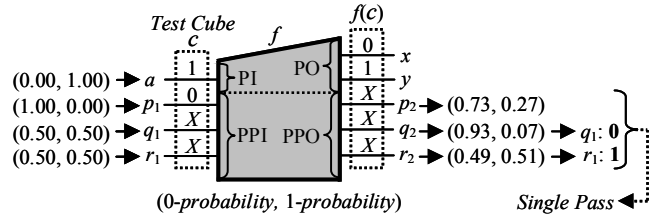

Fig. 9 Probability-Based *X*-Filling.

Thus, there is a need for more balanced *X*-filling, that is highly effective and sufficiently scalable. This is achieved by a new *X*-filling method, called *justification-probability-based fill* (*JP-fill*), whose details are described in Section 5.

3. New Post-ATPG *X*-Filling Scheme

The general flow of the new post-ATPG *X*-filling scheme is shown in Fig. 10. It is a post-processing procedure conducted on an initial transition delay test set V_1, such that the resulting final test set V_2 has lower launch-induced switching activity, thus lower power supply noise.
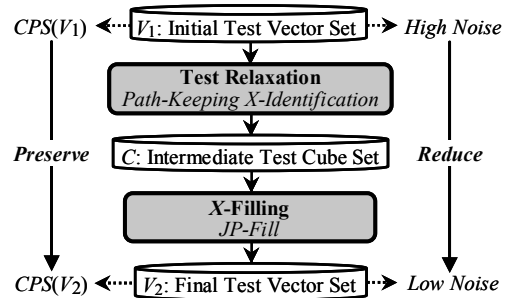
Fig. 10 General Flow of New Post-ATPG *X*-Filling.

The new scheme has two unique characteristics:

(1) **Test Quality Preservation in Test Relaxation**: Delay test quality, as well as fault coverage, of the original test set is preserved, i.e. $CPS(V_2) \geq CPS(V_1)$. This is achieved by *path-keeping X-identification*, to be described in Section 4.

(2) **Balanced Effectiveness and Scalability in *X*-Filling**: The effectiveness and scalability of *X*-filling are achieved in a more balanced manner by *justification-probability-based fill* (*JP-fill*), to be described in Section 5.

4. New Test Relaxation Method

As described in 2.1, the delay test quality of a transition delay test set V is largely determined by its characteristic path set $CPS(V)$. Therefore, test relaxation with the delay test quality preservation capability can be achieved by path-keeping X-identification as stated below:

Path-Keeping X-identification: Given a fully-specified transition delay test set V and its characteristic path set $CPS(V)$, find a partially-specified test cube set C, such that $CPS(C) = CPS(V)$.

Suppose that V_1 is the original fully-specified test set, and C is the partially-specified test cube set obtained by path-keeping X-identification. That is, $CPS(C) = CPS(V_1)$. Also suppose that V_2 is the final fully-specified test set obtained by X-filling C. Since X-filling cannot affect characteristic paths already sensitized by C but may sensitize even longer paths, we have $CPS(C) \leq CPS(V_2)$. As a result, $CPS(V_2) \geq CPS(V_1)$. This means that the delay test quality of V_2, measured by SDQL [4] discussed in Section 2.1, is not lower than that of V_1. Therefore, the delay test quality of V_1, as well as its fault coverage, is preserved by V_2 in post-ATPG X-filling because of path-keeping X-identification.

In the following, we first describe the basic idea of path-keeping X-identification. Then, we present its key operation. Finally, we show its general flow.

4.1 Basic Idea

The relation between V and its characteristic path set $CPS(V)$ can be expressed by a ***sensitization table***, which lists all test vectors and all characteristic paths sensitized by each test vector. An example is shown in Table 1.

Table 1 Sensitization Table

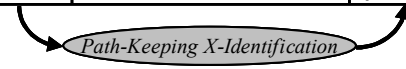| Test Vector	Sensitized Characteristic Paths	
$v_1 = \langle 011 \rangle$	p_1	p_2
$v_2 = \langle 101 \rangle$	p_3	p_4
$v_3 = \langle 111 \rangle$	p_3	p_5

In Table 1, $V = \{v_1, v_2, v_3\}$ and $CPS(V) = \{p_1, p_2, \ldots, p_5\}$. Note that one characteristic path may be sensitized by two or more test vectors. For example, p_3 is sensitized by both v_2 and v_3. However, such cases are seldom for test vectors generated by timing-aware ATPG [2, 9].

The basic idea of path-keeping X-identification is as follows: For each fully-specified test vector v_i in a test vector set $V = \{v_i \mid i = 1, 2, \ldots, n\}$, create a partially-specified test cube c_i, such that c_i sensitizes all characteristic paths sensitized by v_i. Obviously, for the resulting test cube set $C = \{c_i \mid i = 1, 2, \ldots, n\}$, $CPS(C) = CPS(V)$ holds.

Table 2 shows an example of the basic idea, for the test vector set $V = \{v_1, v_2, v_3\}$ given in Table 1. Path-keeping X-identification turns V into the test cube set $C = \{c_1, c_2, c_3\}$, such that c_1 sensitizes p_1 and p_2 as v_1, c_2 sensitizes p_3 and p_4 as v_2, and c_3 sensitizes p_5 as v_3. Obviously, $CPS(C) = \{p_1, p_2, \ldots, p_5\}$. This means that $CPS(C) = CPS(V)$.

Table 2 Example of Basic Idea

Test Vector	Sensitized Characteristic Paths		Test Cube
$v_1 = \langle 011 \rangle$	p_1	p_2	$c_1 = \langle X11 \rangle$
$v_2 = \langle 101 \rangle$	p_3	p_4	$c_2 = \langle 1X1 \rangle$
$v_3 = \langle 111 \rangle$	—	p_5	$c_3 = \langle 1XX \rangle$

Path-Keeping X-Identification

Note that if a characteristic path is sensitized by multiple test vectors, then it will be targeted by just one test vector in test relaxation, so that more X-bits can be identified. In Table 1, for example, p_3 is sensitized by both v_2 and v_3. As shown in Table 2, since c_2 sensitizes both p_3 and p_4, it is only necessary to make c_3 sensitize p_5, instead of both p_3 and p_5. As a result, c_3 contains more X-bits.

4.2 Test Cube Creation

From the basic idea described in Section 4.1, it can be seen that the key operation of path-keeping X-identification is ***test cube creation***. Its purpose is to create a partially-specified test cube c from a fully-specified test vector v, such that c sensitizes all the characteristic paths, $p_1, p_2, \ldots, p_k$, that are originally sensitized by v.

Test cube creation for obtaining such a test cube c is conducted by the following two steps:

Step-1 (***Creating Primary Test Cubes***): k primary test cubes, $c_1, c_2, \ldots, c_k$, are created from the test vector v for the k characteristic paths, $p_1, p_2, \ldots, p_k$, respectively, such that c_i also sensitizes p_i as v does ($i = 1, 2, \ldots, k$).

Step-2 (***Merging Primary Test Cubes***): All primary test cubes, $c_1, c_2, \ldots, c_k$, are merged into a final test cube c, such that c also sensitizes $p_1, p_2, \ldots, p_k$ as v does. Here, c_i sensitizes p_i ($i = 1, 2, \ldots, k$).

The two steps are described in more detail in the following.
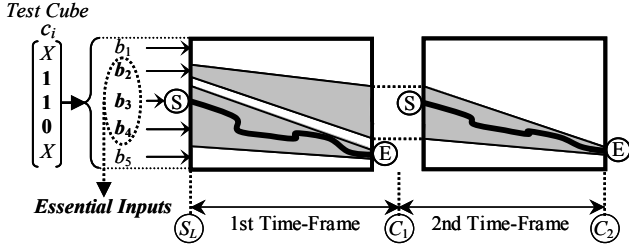
A. Creating Primary Test Cubes

Given a fully-specified test vector v and a characteristic path p_i sensitized by v, a ***primary test cube*** c_i needs to be created from v, such that c_i also sensitizes p_i as v does. This task can be accomplished by a simple but powerful cone-analysis-based technique. An example is shown in Fig. 11.

Fig. 11 (a) shows a full-scan circuit with $b_1, b_2, \ldots, b_5$ as inputs to its combinational portion, and Fig. 11 (b) shows its two-time-frame circuit model for the launch-off-capture-based at-speed scan testing (Fig. 2). A test vector $v = \langle 0\ 1\ 1\ 0\ 1 \rangle$ is applied to $b_1, b_2, \ldots, b_5$. Suppose that v sensitizes the characteristic path p_i, whose start and end points are denoted by S and E, respectively.

In Fig. 11 (b), cone analysis is conducted from the end-point (E) of the characteristic path p_i in both time frames, in order to identify which inputs in $\{b_1, b_2, b_3, b_4, b_5\}$ can affect the sensitization of p_i. Note that the cone analysis from the end-point of p_i in the 2nd time-frame should be conducted in both time-frames as shown in Fig. 11 (b).
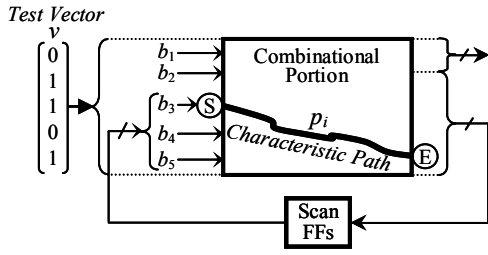
(a) Test vector and sensitized characteristic path

(b) Essential inputs and primary test cube

Fig. 11 Creating a Primary Test Cube.

The result of the cone analysis shows that only b_2, b_3, and b_4 can affect the path p_i for sensitization, and they are called the ***essential inputs*** for the characteristic path p_i. On the other hand, b_1 and b_5 have no impact on p_i, and they are called the ***non-essential inputs*** for the characteristic path p_i. Therefore, the 1st and 5th bits in $v = <0\ 1\ 1\ 0\ 1>$, which correspond to the non-essential inputs b_1 and b_5, respectively, can be turned into X-bits to create a test cube c_i, without affecting the sensitization state of the characteristic path p_i at all. This way, a primary test cube, c_i, is created.

Note that primary test cube creation is based on fast cone analysis to identify X-bits. This makes the process highly efficient even for large industrial circuits. More aggressive techniques based on timing analysis may identify more X-bits, but are too time-consuming to be practical.

B. Merging Primary Test Cubes

Generally, if a test vector v sensitizes k characteristic paths p_1, p_2, …, p_k, the above cone-analysis-based technique can be applied to create k primary test cubes c_1, c_2, …, c_k, respectively. It is obvious that the merged test cube $c = c_1 \cap c_2 … \cap c_k$ also sensitizes p_1, p_2, …, p_k as the test vector v. That is, a final test cube c is created that sensitizes the same set of characteristic paths as the test vector v. This way, test cube creation in path-keeping X-identification is completed.

Note that the $\cap$ operation is a bit-wise operation conducted on a pair of corresponding bits in two test cubes, based on the following rules:

$$X \cap X = X \quad X \cap 0 = 0 \quad X \cap 1 = 1$$

An example is shown in Fig. 12. Here, the test vector $v = <0\ 1\ 1\ 0\ 1>$ sensitizes characteristic paths p_1 and p_2. Two primary test cubes are created: $c_1 = <X\ 1\ 1\ X\ X>$ sensitizes p_1, and $c_2 = <X\ 1\ X\ 0\ X>$ sensitizes p_2. The final test cube is $c = c_1 \cap c_2 = <X\ 1\ 1\ X\ X> \cap <X\ 1\ X\ 0\ X> = <X\ 1\ 1\ 0\ X>$. Obviously, c sensitizes characteristic paths p_1 and p_2 as v.
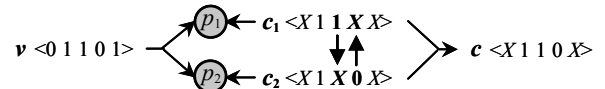

Fig. 12 Merging Primary Test Cubes.

4.3 General Flow

The flow of path-keeping X-identification is shown in Fig. 13. The inputs are a fully-specified test vector set V and its characteristic path set $CPS(V)$, and the output is a partially-specified test cube set C, and $CPS(C) = CPS(V)$.
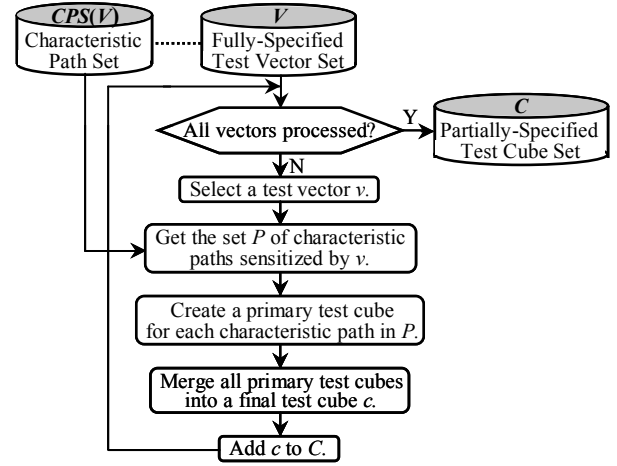

Fig. 13 General Flow of Path-Keeping X-Identification.

The time complexity of path-keeping X-identification is $O(N_1 \times N_2)$, where N_1 is the number of test vectors in V and N_2 is the maximum number of characteristic paths sensitized by a test vector. Since N_2 is small, especially for test vectors generated by timing-aware ATPG [2, 9], it is clear that path-keeping X-identification is efficient and scalable.

5. New X-Filling Method

As described in Section 2.3, justification-based X-filling is effective but less-scalable, while probability-based X-filling is scalable but less-effective. This is tackled by ***justification-probability-based fill*** (***JP-fill***), based on two techniques:

(1) **Limited Justification**: Justification-based X-filling is only conducted for PPI-PPO bit-pairs of the form <logic value, X>, but not for any PPI-PPO bit-pair of the form <X, X> for which multiple passes of justification may be needed. This is to achieve higher scalability.

(2) **Probability Re-Calculation**: Probability-based X-filling is conducted for PPI-PPO bit-pairs of the form <X, X>, but in multiple passes. That is, the logic value for a PPI X-bit is determined only if its corresponding PPO X-bit has significantly different 0 and 1 probabilities; otherwise, probabilities are re-calculated in the next pass. This is to achieve higher effectiveness through improved accuracy.

Obviously, compared to previous X-filling methods based on only justification [19, 21] or only probability (no re-calculation) [22], JP-fill can achieve both effectiveness and scalability in a more balanced manner.

5.1 Circuit Model and Bit-Pairs

Fig. 14 shows the circuit model of LOC-based at-speed scan testing (Fig. 2). c is a test cube, whose PPI part is denoted by <c: PPI>. The response of the combinational portion to c is $f(c)$, whose PPO part is denoted by <$f(c)$: PPO>. When the first capture (C_1 in Fig. 2) is conducted, <$f(c)$: PPO> is loaded into all scan FFs to replace <c: PPI>. This causes launch-induced switching activity.
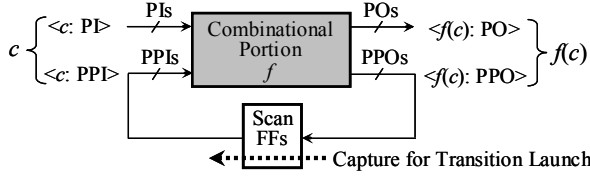
Fig. 14 Circuit Model for Launch-Induced Switching Activity.

The corresponding bits in <c: PPI> and <$f(c)$: PPO> forms a ***bit-pair***, whose types are shown in Table 3. X-filling action for each type of bit-pair in JP-fill is also shown.

Table 3 Types of Bit-Pairs

	<c: PPI> Bit	<$f(c)$: PPO> Bit	X-Filling
Type-A	a	b	*No Action*
Type-B	X_{PPI}	b	*Assignment*
Type-C	a	X_{PPO}	*Justification*
Type-D	X_{PPI}	X_{PPO}	*Probability*

(X_{PPI}: PPI X-bit, X_{PPO}: PPO X-bit, a/b: logic value)

5.2 The General Flow of JP-Fill

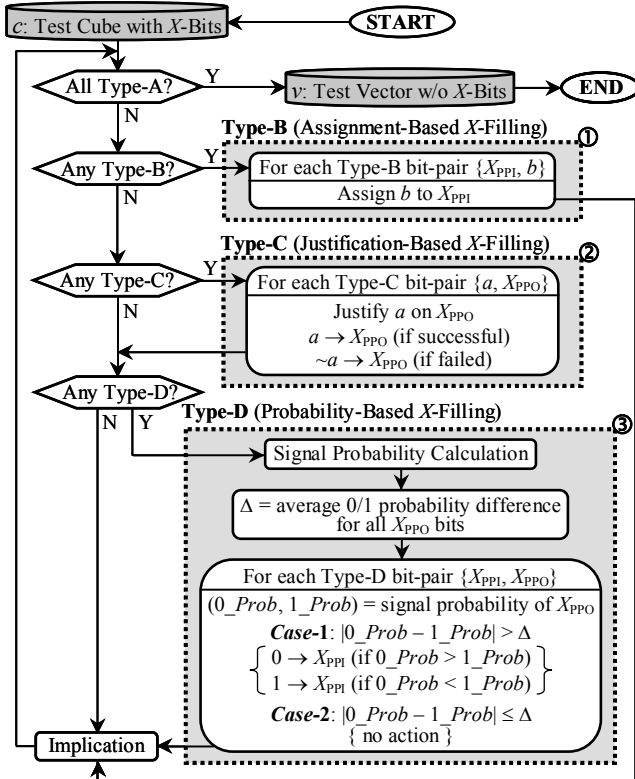The general flow of JP-fill is shown in Fig. 15. The details are described in the following.

Fig. 15 General Flow of JP Fill.

A. Assignment-Based X-Filling

Assignment-based X-filling is conducted on all Type-B bit-pairs first, before any bit-pair of other type is processed.

As shown in Fig. 15-①, for a Type-B X-pair {X_{PPI}, b}, since any value can be set to X_{PPI} by scan shift, logic value b is assigned to X_{PPI} so that a capture transition is avoided.

B. Justification-Based X-Filling

Justification-based X-filling is conducted on all Type-C bit-pairs before Type-D bit-pairs are processed, after all Type-B bit-pairs are processed.

As shown in Fig. 15-②, for a Type-C bit-pair {a, X_{PPO}}, logic value a is justified for the X_{PPO} bit. If this justification succeeds, a is set to X_{PPO}, so that a capture transition is avoided. If this justification fails, ~a is set to X_{PPO}.

C. Probability-Based X-Filling

Probability-based X-filling is conducted on all Type-D bit-pairs after all bit-pairs of other types are processed.

First, the 0 and 1 probabilities, denoted by (0_$Prob$, 1_$Prob$), are calculated for each node. The initial 0 and 1 probabilities for an input with an X-bit are assumed to be 50%, and any probability propagation method can be used [22].

Suppose that the PPO X-bits are X_{PPO}^1, X_{PPO}^2, …, X_{PPO}^m, and that their probabilities are (0_$Prob^1$, 1_$Prob^1$), (0_$Prob^2$, 1_$Prob^2$), …, (0_$Prob^m$, 1_$Prob^m$). The average difference between their 0 and 1 probabilities is calculated as follows:

$$\Delta = (\sum_{i=1}^{m} |0\_Prob^i - 1\_Prob^i|)/m$$

Now consider a Type-D bit-pair {X_{PPI}, X_{PPO}}. Suppose that the 0 and 1 probabilities of X_{PPO} are (0_$Prob$, 1_$Prob$). As shown in Fig. 15-③, different X-filling strategies are used, depending on the relation between 0_$Prob$ and 1_$Prob$:

Case-1 (|0_$Prob$ − 1_$Prob$ | > Δ): In this case, the 0 and 1 probabilities are significantly different at X_{PPO}; thus, the chance of X_{PPO} having the logic value corresponding to the higher probability (0_$Prob$ or 1_$Prob$) is high. Therefore, if 0_$Prob$ > 1_$Prob$, 0 is set to X_{PPI}; otherwise, 1 is set to X_{PPI}. This is the same as the *preferred fill* method [22].

Case-2 (|0_$Prob$ − 1_$Prob$ | ≤ Δ): In this case, the difference between the 0 and 1 probabilities at X_{PPO} is negligibly small, making it inaccurate to use them for determining a logic value for X_{PPI}. Thus, no action is taken. This leads to a new pass of X-filling, in which probabilities are re-calculated to reflect the newly assigned logic values at inputs. As a result, the accuracy of X-filling is improved.

5.3 Summary

In JP-fill, time-consuming justification for Type-D bit-pairs is avoided (Fig. 15-②), and the inaccuracy in probability calculation is alleviated by re-calculation (Fig. 15-③) when 0 and 1 probabilities are so close that proper logic value determination becomes impossible. Thus, more balanced effectiveness and scalability can be achieved by JP-fill.

6. Experimental Results

Path-keeping *X*-identification and JP-fill were implemented in C, and experiments were conducted on 10 ISCAS'89 benchmark circuits on a computer with a 2.6GHz CPU and 16GB memory. The transition delay fault model was used.

A. Test Relaxation Results

Table 4 shows the results of path-keeping *X*-identification on initial test sets generated by two types of ATPG: *timing-ignoring* and *timing-aware* [9], both developed internally. The test vector count, fault coverage, percentage of identified *X*-bits, and CPU time are shown under "Test Vec. #", "Fault Cov. (%)", "*X* (%)", and "CPU (s)", respectively.

From Table 4, it is clear that path-keeping *X*-identification is **effective** in that it identified 54.7% and 67.8% of bits as *X*-bits from fully-specified initial test sets. This method is also **efficient** in that its CPU time was fairly short since the cone-analysis-based technique used is very fast.

Table 4 Results of Path-Keeping *X*-Identification

Circuit	Timing-Ignoring ATPG				Timing-Aware ATPG					
	Test Vec. #	Fault Cov. (%)	*X* (%)	CPU (s)	Test Vec. #	Fault Cov. (%)	*X* (%)	CPU (s)	SDQL Initial	SDQL Final
s1196	26	90.8	41.6	0.0	24	90.8	44.0	0.0	0.26	0.26
s1238	26	90.8	41.6	0.0	24	90.8	41.8	0.0	0.26	0.26
s1423	76	85.8	24.7	0.1	148	85.8	30.4	0.2	1.46	1.45
s5378	178	84.8	53.3	1.0	379	84.8	70.1	2.1	1.52	1.52
s9234	376	81.3	50.8	3.7	839	81.3	64.7	8.2	6.98	6.09
s13207	323	79.5	67.4	4.4	838	79.5	81.3	10.4	7.53	7.53
s15850	221	70.2	54.3	4.0	703	70.2	71.1	10.8	7.33	7.32
s35932	337	82.5	92.0	12.6	763	82.5	94.2	27.0	118.10	117.95
s38417	270	98.0	47.1	12.9	2605	98.0	88.6	93.2	2.39	2.35
s38584	412	83.9	73.9	17.0	2111	83.9	91.8	80.2	4.55	4.53
Ave.	——		54.7	—	——		67.8	—	15.01	14.93

Path-keeping *X*-identification preserves the longest path sensitized by the initial test set for each detected fault when creating the intermediate test cube set. Therefore, the delay test quality, as well as the fault coverage, of the final test set obtained by *X*-filling the intermediate test cube set is guaranteed to be no lower than that of the initial test set.

We used the SDQL metric [4] to quantify the delay test quality of initial and final test sets (obtained by the JP-fill method) for timing-aware ATPG, and the results are also shown in Table 4. It can be seen that the final SDQL values are equal to or even smaller than the values for the initial test sets. This confirms that the delay test quality was not degraded due to test relaxation. Note that the smaller the SDQL value, the higher the delay test quality [4].
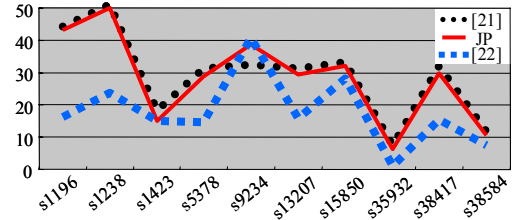
B. X-Filling Results

Table 5 shows the *X*-filling results by a *justification-based* method [21], a *probability-based* method [22], and the *JP-fill* method. Initial test vectors were generated by timing-aware ATPG [9], and test cubes were obtained by path-keeping *X*-identification. The **WSA** (**Weighted Switching Activity**) metric [12, 22] was used for estimating the launch-

induced switching activity at the first capture (C_1 in Fig. 2). Table 5 shows the reduction ratios for maximum WSA at all FFs ("Max. WSA-FF"), maximum WSA at all nodes ("Max. WSA-Node"), average WSA at all nodes ("Ave. WSA-Node"), and the CPU time.

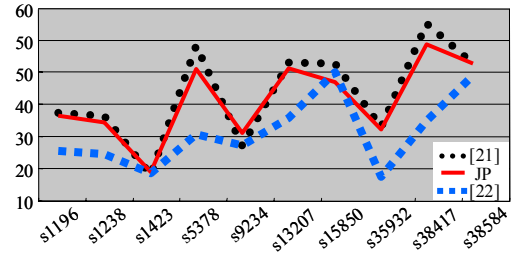**Table 5 Results of Various *X*-Filling Methods**

| Circuit | Reduction Ratio (%) | | | | | | | | | CPU (s) | | |
| | Max. WSA-FF | | | Max. WSA-Node | | | Ave. WSA-Node | | | | | |
	[21]	JP	[22]	[21]	JP	[22]	[21]	JP	[22]	[21]	JP	[22]
s1196	43.2	**43.2**	16.2	33.1	**20.2**	17.2	31.1	**29.8**	16.8	0	**0**	0
s1238	50.0	**50.0**	23.7	29.3	**20.1**	17.1	30.0	**27.5**	15.7	0	**0**	0
s1423	17.1	**14.9**	14.9	6.4	**4.5**	6.8	7.7	**8.7**	8.4	0	**0**	0
s5378	30.1	**28.8**	14.6	16.7	**15.9**	6.4	56.4	**47.5**	23.2	3	**4**	3
s9234	31.2	**38.6**	40.7	7.1	**15.5**	12.3	18.5	**23.4**	18.9	23	**15**	10
s13207	30.1	**29.3**	15.7	24.4	**29.7**	23.2	50.1	**47.7**	29.3	69	**29**	14
s15850	32.1	**32.1**	28.1	21.3	**22.2**	19.1	49.6	**42.5**	46.4	36	**29**	15
s35932	6.2	**6.3**	1.0	7.0	**1.1**	-6.1	25.6	**24.7**	7.1	708	**59**	37
s38417	30.9	**29.8**	15.3	15.4	**14.9**	12.0	64.9	**56.8**	28.0	647	**280**	191
s38584	10.5	**10.5**	7.4	14.2	**14.3**	9.8	49.7	**49.5**	45.2	877	**259**	112
Ave.	28.1	**28.3**	17.8	17.5	**15.8**	11.8	38.3	**35.8**	23.9	——		

(a) Comparison of Max. WSA-FF Reduction
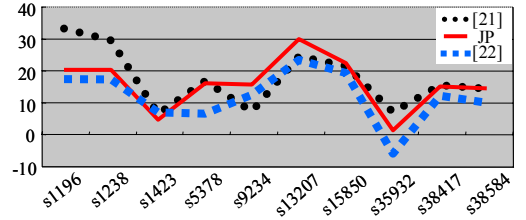
(b) Comparison of Max. WSA-Node Reduction

(c) Comparison of Ave. WSA-Node Reduction
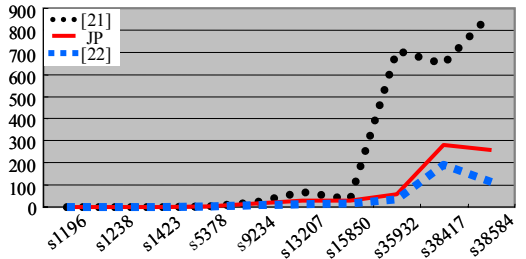
(d) Comparison of CPU time

Fig. 16 Comparison of Various *X*-Filling Methods.

Fig. 16 is the graphical form of the results given in Table 5. The ***effectiveness*** of the *X*-filling methods was evaluated by the launch-induced switching activity at all FFs ("WSA-FF") and all nodes ("WSA-Node"), at maximum and in average, as shown in Fig. 16 (a) ~ (c). The ***scalability*** of the *X*-filling methods was evaluated by CPU time, as shown in Fig. 16 (d). Evidently, the justification-based method [21] is the best-performing for effectiveness, while the probability-based method [22] is the best-performing for scalability.

Fig. 16 (a) ~ (c) also show that, for ***effectiveness***, the JP-fill method is much closer to the best-performing justification-based method [21] than the probability-based method [22]. Fig. 16 (d) also shows that, for ***scalability***, the JP-method is much closer to the best-performing probability-based method [22] than the justification-based method [21]. This confirms that the JP-fill method proposed in this paper can indeed achieve both effectiveness and scalability in a more balanced manner than the previous *X*-filling approaches based on only justification or only probability.

7. Conclusions

This paper proposed a new post-ATPG *X*-filling scheme, featuring two novel and practical methods: (1) ***path keeping X-identification*** for finding don't-care bits from a fully-specified transition delay test set while preserving its delay test quality by keeping the longest paths sensitized for fault detection, and (2) ***justification-probability-based fill*** (***JP-fill***) for *X*-filling test cubes in an effective and scalable manner. This scheme can be easily implemented into any ATPG flow to effectively reduce power supply noise in high-quality at-speed scan testing, without any impact on delay test quality, test data volume, area, and timing.

Experiments on large industrial circuits are currently under way, and the results will be included in the final version. Future research subjects include (I) applying the basic idea and techniques of this paper to path delay test generation, and (II) extending them for test compression schemes.

References

[1] S. Mitra, E. Volkerink, E. McCluskey, and S. Eichenberger, "Delay Defect Screening Using Process Monitor Structures," *Proc. VLSI Test Symp.*, pp. 43-52, 2004.

[2] X Lin, K. Tsai, C. Wang, M. Kassab, J. Rajaski, T. Kobayashi, R. Klingenberg, Y. Sato, S. Hamada, and T. Aikyo, "Timing-Aware ATPG for High Quality At-Speed Testing of Small Delay Defects," *Proc. Asian Test Symp.*, pp.139-146, 2006.

[3] L.-T. Wang, C.-W. Wu, and X. Wen, (Editors), *VLSI Test Principles and Architectures: Design for Testability*, San Francisco: Elsevier, 2006.

[4] Y. Sato, S. Hamada, T. Maeda, A. Takatori, Y. Nozuyama, and S. Kajihara, "Invisible Delay Quality - SDQM Model Lights Up What Could Not Be Seen," *Proc. Int'l Test Conf.*, Paper 47.1, 2005.

[5] N. Ahmed, M. Tehranipoor, and V. Jayaram, "A Novel Framework for Faster-than-at-Speed Delay Test Considering IR-Drop Effects," *Proc. Int'l Conf. on Computer-Aided Design*, pp. 439-444, 2005.

[6] B. Kruseman, A. Majhi, G. Gronthoud, and S. Eichenberger, "On Hazard-Free Patterns for Fine-Delay Fault Testing," *Proc. Int'l Test Conf.*, Paper 9.1, 2004.

[7] Y. Shao, I. Pomeranz, and S. Reddy, "On Generating High Quality Tests for Transition Faults," *Proc. Asian Test Symp.*, pp. 1-8, 2002.

[8] K. Yang, K.-T Cheng, and L.-C Wang, "TranGen: A SAT-Based ATPG for Path-Oriented Transition Faults," *Proc. Asian and South Pacific Design Automation Conf.*, pp. 92-97, 2004.

[9] S. Kajihara, S. Morishima, A. Takuma, X. Wen, T. Maeda, S. Hamada, and Y. Sato, "A Framework of High-Quality Transition Fault ATPG for Scan Circuits," *Proc. Int'l Test Conf.*, Paper 2.1, 2006.

[10] J. Wang, D. M. H. Walker, A. Majhi, B. Kruseman, G. Gronthoud, L. E. Villagra, P. Wiel, and S. Eichenberger, "Power Supply Noise in Delay Testing," *Proc. Int'l Test Conf.*, Paper 17.3, 2006.

[11] J. Saxena, K. M. Butler, V. B. Jayaram, and S. Kundu, "A Case Study of IR-Drop in Structured At-Speed Testing," *Proc. Int'l Test Conf.*, pp. 1098-1104, 2003.

[12] P. Girard, "Survey of Low-Power Testing of VLSI Circuits," *IEEE Design & Test of Computers*, Vol. 19, No. 3, pp. 82-92, May/June 2002.

[13] N. Nicolici and B. Al-Hashimi, *Power-Constrained Testing of VLSI Circuits*, Kluwer Academic Publishers, 2003.

[14] M. Nourani, M. Tehranipoor, and N. Ahmed, "Pattern Generation and Estimation for Power Supply Noise Analysis," *Proc. VLSI Test Symp.*, pp. 439-444, 2005.

[15] A. Kokrady and C. P. Ravikumar, "Fast, Layout-Aware Validation of Test Vectors for Nanometer-Related Timing Failures," *Proc. Int'l Conf. on VLSI Design,* pp. 597-602, 2004.

[16] S. Wang and W. Wei, "A Technique to Reduce Peak Current and Average Power Dissipation in Scan Designs by Limited Capture," *Proc. Asian S. Pacific Design Automation Conf.*, pp. 810-816, 2007.

[17] F. Corno, P. Prinetto, M. Redaudengo, and M. Reorda, "A Test Pattern Generation Methodology for Low Power Consumption," *Proc. VLSI Test Symp.*, pp. 35-40, 1998.

[18] X. Wen, S. Kajihara, K. Miyase, T. Suzuki, K. K. Saluja, L.-T. Wang, K. S. Abdel-Hafez, and K. Kinoshita, "A New ATPG Method for Efficient Capture Power Reduction During Scan Testing," *Proc. VLSI Test Symp.*, pp. 58-63, 2006.

[19] X. Wen, Y. Yamashita, S. Morishima, S. Kajiihara, L.-T. Wang, K. K. Saluja, and K. Kinoshita, "On Low-Capture-Power Test Generation for Scan Testing," *Proc. VLSI Test Symp.*, pp. 265-270, 2005.

[20] W. Li, S. M. Reddy, I. Pomeranz, "On Reducing Peak Current and Power during Test," *Proc. ISVLSI*, pp. 156-161, 2005.

[21] X. Wen, Y. Yamashita, S. Morishima, S. Kajihara, L.-T. Wang, K. K. Saluja, and K. Kinoshita, "Low-Capture-Power Test Generation for Scan-Based At-Speed Testing," *Proc. Int'l Test Conf.*, Paper 39.2, 2005.

[22] S. Remersaro, X. Lin, Z. Zhang, S. M. Reddy, I. Pomeranz, and J. Rajski, "Preferred Fill: A Scalable Method to Reduce Capture Power for Scan Based Designs," *Proc. Int'l Test Conf.*, Paper 32.2, 2006.

[23] X. Wen, K. Miyase, T. Suzuki, Y. Yamato, S. Kajihara, L.-T. Wang, and K. K. Saluja, "A Highly-Guided *X*-Filling Method for Effective Low-Capture-Power Scan Test Generation," *Proc. Int'l Conf.* on Computer Design, pp. 251-258, 2006.

[24] K. M. Butler, J. Saxena, T. Fryars, G. Hetherington, A. Jain, and J. Levis, "Minimizing Power Consumption in Scan Testing: Pattern Generation and DFT Techniques," *Proc. Int'l Test Conf.*, pp. 355-364, 2004.

[25] J. Wang, Z. Yue, X. Lu, W. Qiu, W. Shi, and D. M. H. Walker, "A Vector-Based Approach for Power Supply Noise Analysis in Test Compaction," *Proc. Int'l Test Conf.*, Paper 22.2, 2005.

[26] R. Sankaralingam and N. A. Touba, "Controlling Peak Power during Scan Testing," *Proc. VLSI Test Symp.*, pp. 153-159, 2002.

[27] A. H. El-Maleh and K. Al-Utaibi, "An Efficient Test Relaxation Technique for Synchronous Sequential Circuits," *IEEE Trans. on Computer-Aided Design*, Vol. 23, No. 6, pp. 933-940, June 2004.

[28] K. Miyase and S. Kajihara, "XID: Don't Care Identification of Test Patterns for Combinational Circuits," *IEEE Trans. on Computer-Aided Design*, Vol. 23, No. 2, pp. 321-326, Feb. 2004.